C. R. Mecanique 344 (2016) 631–641

Contents lists available at ScienceDirect

Comptes Rendus Mecanique

www.sciencedirect.com

Free vibration analysis of FG plates resting on an elastic foundation and based on the neutral surface concept using higher-order shear deformation theory

Rabia Benferhat [a], Tahar Hassaine Daouadji [b,*], Mohamed Said Mansour [a]

[a] Laboratoire de géomatériaux, Département de génie civil, Université de Chlef, Algérie
[b] Département de génie civil, Université Ibn-Khaldoun, BP 78 Zaaroura, 14000 Tiaret, Algérie

A R T I C L E   I N F O

Article history:
Received 25 October 2015
Accepted 5 March 2016
Available online 9 July 2016

Keywords:
Functionally graded material
Analytical solution
Free vibration analysis
Neutral surface concept
Elastic foundation

A B S T R A C T

An analytical solution based on the neutral surface concept is developed to study the free vibration behavior of a simply supported functionally graded plate reposing on the elastic foundation by taking into account the effect of transverse shear deformations. No transversal shear correction factors are needed because a correct representation of the transversal shearing strain obtained by using a new refined shear deformation theory. The foundation is described by the Winkler–Pasternak model. The Young's modulus of the plate is assumed to vary continuously through the thickness according to a power law formulation, and the Poisson ratio is held constant. The equation of motion for FG rectangular plates resting on an elastic foundation is obtained through Hamilton's principle. Numerical examples are provided to show the effect of foundation stiffness parameters presented for thick to thin plates and for various values of the gradient index, aspect, and the side-to-thickness ratio. It was found that the proposed theory predicts the fundamental frequencies very well, consistently with those available in the literature.

1. Introduction

The technique of grading ceramics along with metals initiated by Japanese material scientists in Sendai has marked the beginning of the exploration of the possibility of using FGMs for various structural applications [1]. Since then, an effort has been devoted to the development of high-performance heat-resistant functionally graded materials. FGMs are therefore composite materials with a microscopically inhomogeneous character. Continuous changes in their microstructure make FGMs distinguish from conventional composite materials. Functionally graded materials (FGM) structures are those in which the volume fractions of two or more materials are varied continuously as a function of their position along certain dimension(s) of the structure to achieve a required function. Typically, FGMs are made from a mixture of ceramic and metal. It is difficult to obtain an exact enough solution to the nonlinear equations to develop efficient mathematical models to predict the static and dynamic response of a plate. Thus far, only a few exact solutions have been investigated. However, with progress in science and technology, a need arises in engineering practice to accurately predict the nonlinear static and dynamic responses of a plate.

* Corresponding author. Tel.: +213 46 42 93 77; fax: +213 46 42 87 38.
E-mail address: daouadjitah@yahoo.fr (T. Hassaine Daouadji).

http://dx.doi.org/10.1016/j.crme.2016.03.002
1631-0721/

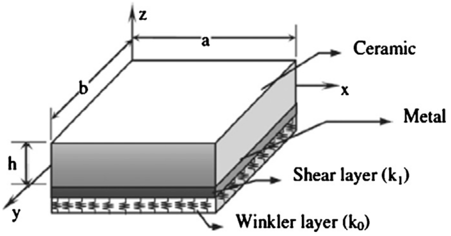

Fig. 1. Geometry and dimensions of the FGM plate resting on an elastic foundation.

Plates supported by elastic foundations have been widely adopted by many researchers to model various engineering problems during the past decades. To describe the interactions of the plate and its foundation as appropriately as possible, scientists have proposed various kinds of foundation models [2]. The simplest model for the elastic foundation is the Winkler model, which regards the foundation as a series of separated springs without coupling effects between each other, resulting in the disadvantage of discontinuous deflection on the interacted surface of the plate. This was later improved by Pasternak [3], who exploited the interactions between the separated springs in the Winkler model by introducing a new dependent parameter. From then on, the Pasternak model was widely used to describe the mechanical behavior of structure–foundation interactions [4,5].

Several investigations have been presented for the analysis of FG plates. Reddy [6] thermomechanical loads, theoretical formulation, Navier's solution and finite element model for the FG plate were presented. Vel et al. [7] provided an exact solution for three-dimensional deformations of a simply supported functionally graded rectangular plate subjected to mechanical and thermal loads on its top and/or bottom surfaces. Talha et al. [8] established free vibration and static analysis of functionally graded material (FGM) plates using higher-order shear deformation theory with a special modification in the transverse displacement in conjunction with finite element models. Ferreira et al. [9] analyzed the static deformations of a simply supported functionally graded plate modeled by a third-order shear deformation theory using the collocation multiquadric radial basis functions. Ramirez et al. [10] gave an approximate solution for the static analysis of three-dimensional, anisotropic, elastic plates composed of functionally graded materials by using a discrete layer theory in combination with the Ritz method in which the plate is divided into an arbitrary number of homogeneous and/or FGM layers. Park et al. [11] presented thermal postbuckling and vibration behaviors of the functionally graded (FG) plate, the nonlinear finite element equations being based on the first-order shear deformation plate theory and the von Karman nonlinear strain–displacement relationship being used to account for the large deflection of the plate.

The objective of this investigation is to present a new refined shear deformation theory to study the free vibration behavior of a simply supported functionally graded plate reposing on the elastic foundation using an analytical solution procedure based on the neutral surface concept. This theory does not require shear correction factors and just four unknown displacement functions are used against five or more unknown displacement functions used in the corresponding ones. The obtained results have been compared with the ones available in the literature and were found to be in good agreement with them.

2. Geometric configuration and material properties

The FGM plate is regarded to be a single layer plate of uniform thickness. Here the FGM is a plate of length a, width b, and total thickness h made from anisotropic material of metal and ceramics, in which the composition varies from the top to the bottom surface. To specify the position of the neutral surface of FG plates, two different planes are considered for the measurement of z, namely z_{ms} and z_{ns} measured from the middle surface and the neutral surface of the plate, respectively, as shown in Fig. 1.

The volume fraction of ceramic (V_{c}) can be written in terms of z_{ms} and z_{ns} coordinates as [12]:

$$V_{\mathrm{c}}(z) = \left(\frac{z_{\mathrm{ms}}}{h} + \frac{1}{2}\right)^k = \left(\frac{z_{\mathrm{ns}} + c}{h} + \frac{1}{2}\right)^k \tag{1}$$

where h is the thickness of the plate and k denotes the power of the FGM, which takes values greater than or equal to zero. Also, the parameter C is the distance from the neutral surface to the middle surface. The volume fraction of metal is expressed as:

$$V_{\mathrm{m}}(z) = 1 - V_{\mathrm{c}}(z) \tag{2}$$

The effective Young's modulus E is expressed as [13]:

$$E(z) = E_{\mathrm{m}} V_{\mathrm{m}}(z) + E_{\mathrm{c}} V_{\mathrm{c}}(z) \tag{3}$$

where E_{m} and E_{c} are Young's moduli of the metal and of the ceramic, respectively. The position of the neutral surface of the FG plate is determined to satisfy the first moment with respect to Young's modulus, being zero as follows [13]:

$$\int_{-h/2}^{h/2} E(z_{\text{ms}})(z_{\text{ms}} - C)\mathrm{d}z_{\text{ms}} = 0 \tag{4}$$

Consequently, the position of neutral surface can be obtained as

$$C = \frac{\int_{-h/2}^{h/2} E(z_{\text{ms}}) z_{\text{ms}} \mathrm{d}z_{\text{ms}}}{\int_{-h/2}^{h/2} E(z_{\text{ms}}) \mathrm{d}z_{\text{ms}}} \tag{5}$$

It can be seen that the physical neutral surface and the geometric middle surface are the same in a homogeneous isotropic plate.

3. Displacement field and strains

In the present study, the system of governing equations for FGM plate is derived by using the variational approach. The origin of the material coordinates is at the neutral surface of the plate as shown in Fig. 1. The in-plane displacements and the transverse displacement for the plate are assumed to be:

$$\begin{aligned}
u(x, y, z_{\text{ns}}) &= u_0(x, y) - z_{\text{ns}} \frac{\partial w_{\text{b}}}{\partial x} - f(z_{\text{ns}}) \frac{\partial w_{\text{s}}}{\partial x} \\
v(x, y, z_{\text{ns}}) &= v_0(x, y) - z_{\text{ns}} \frac{\partial w_{\text{b}}}{\partial y} - f(z_{\text{ns}}) \frac{\partial w_{\text{s}}}{\partial y} \\
w(x, y, z_{\text{ns}}) &= w_{\text{b}}(x, y) + w_{\text{s}}(x, y)
\end{aligned} \tag{6}$$

where $f(z_{\text{ns}})$ represents shape functions determining the distribution of the transverse shear strains and stresses along the thickness and is given as

$$f(z_{\text{ns}}) = z_{\text{ns}} + C - \sin\left(\frac{\pi(z_{\text{ns}} + C)}{h}\right) \tag{7}$$

It should be noted that unlike the first-order shear deformation theory, this theory does not require shear correction factors. The kinematic relations can be obtained as follows:

$$\begin{aligned}
\varepsilon_x &= \varepsilon_x^0 + z_{\text{ns}} k_x^b + f(z_{\text{ns}}) k_x^s \\
\varepsilon_y &= \varepsilon_y^0 + z_{\text{ns}} k_y^b + f(z_{\text{ns}}) k_y^s \\
\gamma_{xy} &= \gamma_{xy}^0 + z_{\text{ns}} k_{xy}^b + f(z_{\text{ns}}) k_{xy}^s \\
\gamma_{yz} &= g(z_{\text{ns}}) \gamma_{yz}^s \\
\gamma_{xz} &= g(z_{\text{ns}}) \gamma_{xz}^s \\
\varepsilon_z &= 0
\end{aligned} \tag{8}$$

where

$$\begin{aligned}
&\varepsilon_x^0 = \frac{\partial u_0}{\partial x}, \quad k_x^b = -\frac{\partial^2 w_b}{\partial x^2}, \quad k_x^s = -\frac{\partial^2 w_s}{\partial x^2}, \quad \varepsilon_y^0 = \frac{\partial v_0}{\partial y}, \quad k_y^b = -\frac{\partial^2 w_b}{\partial y^2}, \quad k_y^s = -\frac{\partial^2 w_s}{\partial y^2} \\
&\gamma_{xy}^0 = \frac{\partial u_0}{\partial y} + \frac{\partial v_0}{\partial x}, \quad k_{xy}^b = -2\frac{\partial^2 w_b}{\partial x \partial y}, \quad k_{xy}^s = -2\frac{\partial^2 w_s}{\partial x \partial y}, \quad \gamma_{yz}^s = \frac{\partial w_s}{\partial y}, \quad \gamma_{xz}^s = \frac{\partial w_s}{\partial x} \\
&g(z_{\text{ns}}) = 1 - f'(z_{\text{ns}}) \quad \text{and} \quad f'(z_{\text{ns}}) = \frac{\mathrm{d}f(z_{\text{ns}})}{\mathrm{d}z_{\text{ns}}}
\end{aligned} \tag{9}$$

The constitutive relation describes how the stresses and strains are related within the plate and is expressed as

$$\begin{aligned}
&\begin{Bmatrix} \sigma_x \\ \sigma_y \\ \tau_{xy} \end{Bmatrix} = \begin{bmatrix} Q_{11} & Q_{12} & 0 \\ Q_{12} & Q_{22} & 0 \\ 0 & 0 & Q_{66} \end{bmatrix} \begin{Bmatrix} \varepsilon_x \\ \varepsilon_y \\ \gamma_{xy} \end{Bmatrix} \\
&\begin{Bmatrix} \tau_{yz} \\ \tau_{zx} \end{Bmatrix} = \begin{bmatrix} Q_{44} & 0 \\ 0 & Q_{55} \end{bmatrix} \begin{Bmatrix} \gamma_{yz} \\ \gamma_{zx} \end{Bmatrix}
\end{aligned} \tag{10}$$

where $(\sigma_x, \sigma_y, \tau_{xy}, \tau_{xz}, \tau_{yz})$ are the stress components; $(\varepsilon_x, \varepsilon_y, \gamma_{xy}, \gamma_{xz}, \gamma_{yz})$ are the strain components; Q_{ij} are the plane stress-reduced stiffness values, which can be calculated by

$$Q_{11} = Q_{22} = \frac{E(z_{\text{ns}})}{1 - \nu^2}, \quad Q_{12} = \frac{\nu E(z_{\text{ns}})}{1 - \nu^2}, \quad Q_{44} = Q_{55} = Q_{66} = \frac{E(z_{\text{ns}})}{2(1 + \nu)} \tag{11}$$

3.1. Governing equations and boundary conditions

Hamilton's principle is used herein to derive the equations of motion appropriate to the displacement field and the constitutive equations. The principle can be stated in analytical form as:

$$0 = \delta \int_{t_1}^{t_2} (U + U_{\mathrm{F}} - K - W)\mathrm{d}t \tag{12}$$

where U is the strain energy and K is the kinetic energy of the FG plate, U_{F} is the strain energy of foundation and W is the work of external forces. Employing the minimum of the total energy principle leads to a general equation of motion and boundary conditions. Taking the variation of the above equation and integrating by parts:

$$\int_{t_1}^{t_2} \left[\int_V [\sigma_x \delta\varepsilon_x + \sigma_y \delta\varepsilon_y + \tau_{xy}\delta\gamma_{xy} + \tau_{yz}\delta\gamma_{yz} + \tau_{zx}\delta\gamma_{zx} - \rho(\ddot{u}\delta u + \ddot{v}\delta v + \ddot{w}\delta w)\mathrm{d}v + \int_A [f_e \delta w]\mathrm{d}A \right]\mathrm{d}t = 0 \tag{13}$$

where (13) represents the second derivative with respect to time and f_{e} is the density of reaction force of foundation. For the Pasternak foundation model:

$$f_{\mathrm{e}} = k_0 w - k_1 \nabla^2 w \tag{14}$$

If the foundation is modeled as the linear Winkler foundation, the coefficient k_1 in Eq. (14) is zero. Using Eq. (8), Eq. (13) takes the following form:

$$\begin{aligned}
&\int_{t_1}^{t_2} \Bigg[\int_A \big\{ \delta u N_{x,x} + \delta v N_{y,y} + \delta u N_{xy,y} + \delta v N_{xy,x} - \delta w M_{y,yy} - 2\delta w M_{xy,xy} + \delta\theta_x P_{x,x} + \delta\theta_y P_{y,y} + \delta\theta_x P_{xy,y} \\
&\quad + \delta\theta_y P_{xy,x} + \delta\theta_y(-R) + \delta\theta_x(-R) \big\}\mathrm{d}A + \int_A f_{\mathrm{e}}\delta w \mathrm{d}A - \int_A \big\{ \delta u(I_1\ddot{u} - I_2\ddot{w}_{,x} + I_4\ddot{\theta}_x) + \delta v(I_1\ddot{v} - I_2\ddot{w}_{,y} + I_4\ddot{\theta}_y) \\
&\quad + \delta w(I_1\ddot{w} + I_2\ddot{u}_{,x} - I_3\ddot{w}_{,xx} + I_5\ddot{\theta}_{x,x} + I_2\ddot{v}_{,y} - I_3\ddot{w}_{,yy} - I_5\ddot{\theta}_{y,y}) + \delta\theta_x(I_4\ddot{u} - I_5\ddot{w}_{,x} + I_6\ddot{\theta}_x) \\
&\quad + \delta\theta_y(I_4\ddot{v} - I_5\ddot{w}_{,y} + I_6\ddot{\theta}_y)\mathrm{d}A \big\} \Bigg]\mathrm{d}t = 0
\end{aligned} \tag{15}$$

where stress and moment resultants are defined as:

$$\begin{aligned}
&\begin{Bmatrix} N \\ M \\ P \end{Bmatrix} = \begin{bmatrix} A_{ij} & B_{ij} & C_{ij} \\ B_{ij} & D_{ij} & E_{ij} \\ C_{ij} & E_{ij} & C_{ij} \end{bmatrix} \begin{Bmatrix} \varepsilon \\ k \\ k_0 \end{Bmatrix} \quad (i, j = 1, 2, 6) \\
&\{R\} = [F_{ij}]\{\theta\} \quad (i, j = 4, 5)
\end{aligned} \tag{16}$$

in which:

$$\begin{aligned}
&\varepsilon = \begin{Bmatrix} u_{0,x} \\ v_{0,y} \\ u_{0,y} + v_{0,x} \end{Bmatrix}, \qquad k = -\begin{Bmatrix} w_{,xx} \\ w_{,xx} \\ 2w_{,xy} \end{Bmatrix} \\
&k_0 = \begin{Bmatrix} \theta_{x,x} \\ \theta_{y,y} \\ \theta_{x,y} + \theta_{y,x} \end{Bmatrix}, \qquad \theta = \begin{Bmatrix} \theta_x \\ \theta_y \end{Bmatrix}
\end{aligned} \tag{17}$$

and stiffness components and inertias are given as:

$$\{A_{ij}, B_{ij}, C_{ij}, D_{ij}, E_{ij}, G_{ij}\} = \int_{-h/2-c}^{h/2-c} \left\{1, z_{\mathrm{ns}}, f(z_{\mathrm{ns}}), z_{\mathrm{ns}}^2, z_{\mathrm{ns}} f(z_{\mathrm{ns}}), \left[f(z_{\mathrm{ns}})\right]^2\right\} Q_{ij}\mathrm{d}z_{\mathrm{ns}} \quad (i, j = 1, 2, 6) \tag{18}$$

$$\{F_{ij}\} = \int_{-h/2-c}^{h/2-c} \left[f'(z_{\mathrm{ns}})\right]^2 Q_{ij}\mathrm{d}z_{\mathrm{ns}} \quad (i, j = 1, 2, 6) \tag{19}$$

$$I_1, I_2, I_3, I_4, I_5, I_6 = \int_{-h/2-c}^{h/2-c} \rho\big(1, z_{\mathrm{ns}}, z_{\mathrm{ns}}^2, f(z_{\mathrm{ns}}), z_{\mathrm{ns}} f(z_{\mathrm{ns}}), \big[f(z_{\mathrm{ns}})\big]^2\big)\mathrm{d}z_{\mathrm{ns}} \tag{20}$$

Using the generalized displacement–strain relations and stress–strain relations, and the fundamentals of calculus of variations and collecting the coefficients of δu, δv, δw, $\delta\theta_x$ and $\delta\theta_y$ in Eq. (13), the equations of motion are obtained as:

$$\begin{aligned}
&N_{x,x} + N_{xy,y} = I_1\ddot{u} - I_2\ddot{w}_{,x} + I_4\ddot{\theta}_x \\
&N_{xy,x} + N_{y,y} = I_1\ddot{v} - I_2\ddot{w}_{,y} + I_4\ddot{\theta}_y \\
&M_{x,xx} + 2M_{xy,xy} + M_{y,yy} + k_0 w - k_1\nabla^2 w = I_1\ddot{w} - I_2(\ddot{u}_{,x} + \ddot{v}_{,y}) - I_3(\ddot{w}_{,xx} + \ddot{w}_{,yy}) + I_5(\ddot{\theta}_{x,x} + \ddot{\theta}_{y,y}) \\
&P_{x,x} + P_{xy,y} - R_x = I_4\ddot{u} - I_5\ddot{w}_{,x} + I_6\ddot{\theta}_x \\
&P_{xy,x} + P_{y,y} - R_y = I_4\ddot{v} - I_5\ddot{w}_{,y} + I_6\ddot{\theta}_y
\end{aligned} \tag{21}$$

For the analytical solution to Eq. (21), the Navier method, based on double Fourier series, is used under the specified boundary conditions. Using Navier's procedure, the displacement variables satisfying the above boundary conditions can be expressed in the following Fourier series:

$$\begin{aligned}
u(x,y) &= \sum_{m=1}^{\infty}\sum_{n=1}^{\infty} A_{mn}\cos\frac{m\pi x}{a}\sin\frac{n\pi y}{b}\mathrm{e}^{\mathrm{i}\omega t} \\
v(x,y) &= \sum_{m=1}^{\infty}\sum_{n=1}^{\infty} B_{mn}\sin\frac{m\pi x}{a}\cos\frac{n\pi y}{b}\mathrm{e}^{\mathrm{i}\omega t} \\
w(x,y) &= \sum_{m=1}^{\infty}\sum_{n=1}^{\infty} C_{mn}\sin\frac{m\pi x}{a}\cos\frac{n\pi y}{b}\mathrm{e}^{\mathrm{i}\omega t} \\
\theta_x &= \sum_{m=1}^{\infty}\sum_{n=1}^{\infty} T_{xmn}\cos\frac{m\pi x}{a}\sin\frac{n\pi y}{b}\mathrm{e}^{\mathrm{i}\omega t} \\
\theta_y &= \sum_{m=1}^{\infty}\sum_{n=1}^{\infty} T_{ymn}\sin\frac{m\pi x}{a}\cos\frac{n\pi y}{b}\mathrm{e}^{\mathrm{i}\omega t}
\end{aligned} \tag{22}$$

where A_{mn}, B_{mn}, C_{mn}, T_{xmn}, T_{ymn} are arbitrary parameters to be determined, and ω is the eigenfrequency associated with the (m,n)th eigenmode.

The displacement functions given in Eq. (21) satisfy the kinematic boundary conditions of the simply supported plate, which are given below:

$$\begin{aligned}
&N_x = v = w = M_x = P_x = \theta_y = 0 \quad \text{at } x = 0, a \\
&N_y = u = w = M_y = P_y = \theta_x = 0 \quad \text{at } y = 0, b
\end{aligned} \tag{23}$$

Substituting Eqs. (18), (19), (20), and (22) into equations of motion (21), we get the below eigenvalue equations for any fixed value of m and n, for the free vibration problem:

$$([K] - \omega^2[M]\{\Delta\} = \{0\} \tag{24}$$

where $[K]$ and $[M]$ are stiffness and mass matrices, respectively, and represented as:

$$[K] = \begin{bmatrix} a_{11} & a_{12} & a_{13} & a_{14} & a_{15} \\ a_{12} & a_{22} & a_{23} & a_{24} & a_{25} \\ a_{13} & a_{23} & a_{33} & a_{34} & a_{35} \\ a_{14} & a_{24} & a_{34} & a_{44} & a_{45} \\ a_{15} & a_{25} & a_{35} & a_{45} & a_{55} \end{bmatrix} \tag{25}$$

$$[M] = \begin{bmatrix} I_1 & 0 & -\alpha I_2 & I_4 & 0 \\ 0 & I_1 & -\beta I_2 & 0 & I_4 \\ -\alpha I_2 & -\beta I_2 & I_3(\alpha^2+\beta^2) + I_1 & -\alpha I_5 & -\beta I_5 \\ I_4 & 0 & -\alpha I_5 & I_6 & 0 \\ 0 & I_4 & -\beta I_5 & 0 & I_6 \end{bmatrix} \tag{26}$$

in which:

$$
\begin{aligned}
&a_{11} = A_{11}\alpha^2 + A_{66}\beta^2 \\
&a_{12} = \alpha\beta(A_{12} + A_{66}) \\
&a_{13} = -B_{11}a^3 \\
&a_{14} = C_{11}a^2 + C_{66}\beta^2 \\
&a_{15} = \alpha\beta(C_{12} + C_{66}) \\
&a_{22} = A_{66}\alpha^2 + A_{22}\beta^2 \\
&a_{23} = -B_{22}\beta^3 \\
&a_{24} = \alpha\beta(C_{12} + C_{66}) \\
&a_{25} = C_{66}\alpha^2 + C_{22}\beta^2 \\
&a_{33} = D_{11}\alpha^4 + 2D_{12}\alpha^2\beta^2 + 4D_{66}\alpha^2\beta^2 + D_{22}\beta^4 + k_0 + k_1(\alpha^2 + \beta^2) \\
&a_{34} = -E_{11}\alpha^3 - E_{12}\alpha\beta^2 - 2E_{66}\alpha\beta^2 \\
&a_{35} = -E_{12}\alpha^2\beta - 2E_{66}\alpha^2\beta - E_{22}\beta^3 \\
&a_{44} = F_{55} + G_{11}\alpha^2 + G_{66}\beta^2 \\
&a_{45} = \alpha\beta(G_{12} + G_{66}) \\
&a_{55} = F_{44} + G_{66}\alpha^2 + G_{22}\beta^2
\end{aligned}
\tag{27}
$$

and $\alpha = m\pi/a$, $\beta = n\pi/b$.

The natural frequencies of FG plate can be found from the nontrivial solution to Eq. (24).

4. Numerical results and discussion

In this section, various numerical examples are presented and discussed to verify the accuracy of the present theory in predicting the frequency of simply supported FG plates based on the neutral surface concept. For numerical results, an Al/Al_2O_3 or Al/ZrO_2 plate composed of aluminum (as metal) and alumina or zirconia (as ceramic) is considered. The material properties assumed in the present analysis are as follows:

ceramic (P_C: alumina, Al_2O_3): $E_c = 380$ GPa, $\rho_c = 3800$ kg/m^3

(P_C: zirconia, ZrO_2): $E_c = 200$ GPa, $\rho_c = 5700$ kg/m^3

metal (P_M: aluminum, Al): $E_m = 70$ GPa, $\rho_m = 2700$ kg/m^3

Poisson's ratio is 0.3 for both alumina and aluminum. And their properties change through the thickness of the plate according to a power law. The bottom surfaces of the FG plate are aluminum rich, whereas the top surfaces of the FG plate are alumina or zirconia rich.

For verification purposes, the obtained results are compared with those of Hosseini-Hashemi et al. [14] based on an exact closed-form Levy-type solution. Those of Zhou et al. [15] were based on a three-dimensional Ritz method, those of Matsunaga [16] were based on the higher-order shear deformation theories, whereas the three-dimensional exact solutions of Leissa [17], Liu and Liew [18] were based on a differential quadrature element method and others available in the literature.

In all examples, no transversal shear correction factors are used because a correct representation of the transversal shearing strain is given. For the sake of convenience, the following results are presented in graphical and tabular forms. To illustrate the accuracy of the present theory for FG SSSS square plates made of Al/Al_2O_3 and Al/ZrO_2 for a wide range of power-law indices k and thickness ratios h/a, the variations of non-dimensional natural frequencies and of the fundamental frequency are illustrated in the following examples.

Table 1 shows the comparison of the fundamental frequency parameter ($\overline{w} = \omega h\sqrt{\rho_c/E_c}$) for SSSS Al/Al_2O_3 square plates with three values of the thickness-to-length ratio ($h/a = 0.05, 0.1$ and 0.2). It can be seen that the proposed refined theory using an analytical solution based on the neutral surface concept and the others theories give identical results for all values of the power-law index k. The capability of the present solution is also tested for two types of materials, the plates made of Al/Al_2O_3 and Al/ZrO_2 for a wide range of power-law indices k in Table 2. A close correlation is achieved. Table 3 examines the effect of the thickness-to-length ratio h/a on the first eight non-dimensional natural frequencies $\overline{w} = \omega a^2\sqrt{\rho h/D}$ for simply supported isotropic square plate. As can be seen from the table, not only for thin plates but also for thick plates, the natural frequencies are predicted as accurately by the present method.

Tables 4 and 5 show the comparison of fundamental frequency $\overline{w} = \omega a^2\sqrt{\rho h/D}$ of FG rectangular plates on their elastic foundation with those reported by Akhavan et al., Hassen Ait Atmane et al., Matsunaga and Thai et al., with different values of the thickness-to-length ratios and of foundation stiffness parameters. It can be seen that the results are in excellent agreement with each other. Fundamental frequencies $\overline{w} = \omega b^2\sqrt{SH/A}/\pi^2$ of the FG square plate ($a/b = 1$) with simply-supported boundary conditions for $h/a = 0.01$, 0.1, and 0.2 are listed in Table 6 for different values of the foundation

Table 1
Comparison of fundamental frequency parameters $\overline{w} = \omega h \sqrt{\rho_c / E_c}$ for SSSS Al/Al_2O_3 square plates ($a/b = 1$).

Thickness-to-length ratio h/a	Method	Gradient index k			
		0	1	4	10
0.05	Hosseini-Hashemi [14]	0.01480	0.01150	0.01013	0.00963
	Matsunaga [16]	–	–	–	–
	Zhao [19]	0.01464	0.01118	0.00970	0.00931
	Present	0.01479	0.00997	0.00883	0.00810
0.1	Hosseini-Hashemi [14]	0.05769	0.04454	0.03825	0.03627
	Matsunaga [16]	0.05777	0.04427	0.03811	0.03642
	Zhao [19]	0.05673	0.04346	0.03757	0.03591
	Present	0.05769	0.03913	0.03443	0.03150
0.2	Hosseini-Hashemi [14]	0.2112	0.1650	0.1371	0.1304
	Matsunaga [16]	0.2121	0.1640	0.1383	0.1306
	Zhao [19]	0.2055	0.1587	0.1356	0.1284
	Present	0.2112	0.1460	0.1255	0.1142

Table 2
Comparison of fundamental frequency parameters $\overline{w} = \omega a^2 \sqrt{\rho_c / E_c}/h$ for SSSS square plates ($a/b = 1$) when $h/a = 0.1$.

FGMs	Method	Gradient index k					
		0	1	2	5	8	10
Al/Al_2O_3	Hosseini-Hashemi [14]	5.7693	4.4545	4.0063	3.7837	3.6830	3.6277
	Zhao [19]	5.6763	4.3474	3.9474	3.7218	3.6410	3.5923
	Present	5.7696	3.9138	3.7034	3.3635	3.2093	3.1500
Al/ZrO_2	Hosseini-Hashemi [14]	5.7693	5.2532	5.3084	5.2940	5.2312	5.1893
	Zhao [19]	5.6763	4.8713	4.6977	4.5549	4.4741	4.4323
	Present	5.7696	5.0800	5.1148	5.1381	5.1156	5.1000

Table 3
Comparison of non-dimensional natural frequencies $\overline{w} = \omega a^2 \sqrt{\rho h / D}$ for a simply supported isotropic square plate.

Thickness-to-length ratio h/a	Method	Mode							
		1,1	1,2	2,1	2,2	3,1	1,3	3,2	2,3
0.001	Leissa [17]	19.7392	49.348	49.348	78.9568	98.696	98.696	128.3021	128.3021
	Zhou et al. [15]	19.7115	49.347	49.347	78.9528	98.6911	98.6911	128.3048	128.3048
	Akavci [20]	19.7391	49.3476	49.3476	78.9557	98.6943	98.6943	128.3020	128.3020
	Present	19.7391	49.3475	49.3475	78.9556	98.6942	98.6942	128.3018	128.3018
0.01	Liu et al. [18]	19.7319	49.3027	49.3027	78.8410	98.5150	98.5150	127.9993	127.9993
	Nagino et al.	19.732	49.305	49.305	78.846	98.525	98.525	128.01	128.01
	Akavci [20]	19.7322	49.3045	49.3045	78.8456	98.5223	98.5223	128.012	128.012
	Present	19.7320	49.3032	49.3032	78.8422	98.5171	98.5171	128.0027	128.0027
0.1	Liu et al. [18]	19.0584	45.4478	45.4478	69.7167	84.9264	84.9264	106.5154	106.5154
	Hosseini et al. [14]	19.0653	45.4869	45.4869	69.8093	85.0646	85.0646	106.7350	106.7350
	Akavci [20]	19.0850	45.5957	45.5957	70.0595	85.4315	85.4315	107.3040	107.3040
	Present	19.0660	45.4917	45.4917	69.8212	85.0829	85.0829	106.7652	106.7652
0.2	Shufrin et al.	17.4524	38.1884	38.1884	55.2539	65.3130	65.3130	78.9864	78.9864
	Hosseini et al. [14]	17.4523	38.1883	38.1883	55.2543	65.3135	65.3135	78.9865	78.9865
	Akavci [20]	17.5149	38.4722	38.4722	55.8358	66.1207	66.1207	80.1637	80.1637
	Present	17.4553	38.2052	38.2052	55.2943	65.3731	65.3731	79.0812	79.0812

stiffness parameters, and are computed and compared with other published data. It can be seen from the table that a good agreement is achieved between the results of the present theory and those of other theories.

Figs. 1 and 2 contain the plots of non-dimensional fundamental frequency $\overline{w} = \omega a^2 / h \sqrt{\rho_m / E_m}$ of Al/Al_2O_3 functionally graded square plates with respect to the power-law index k ($k = 0$ to 10) without the elastic foundation ($K_0 = K_1 = 0$). It is clear that the increase in the power-law index k causes a decrease in the non-dimensional fundamental frequency. The latter increases when the aspect and side-to-thickness ratios increase.

Figs. 3 and 4 display the variation of the non-dimensional fundamental frequency $\overline{w} = \omega a^2 / h \sqrt{\rho_m / E_m}$ of Al/Al_2O_3 functionally graded square plates with respect to the power-law index k ($k = 0$ to 10) resting on Winkler and Winkler–Pasternak foundations, respectively. It can be observed that the frequencies increase with the increase in the foundation parameters.

Table 4
Comparison of fundamental frequency parameters $\overline{w} = \omega a^2 \sqrt{\rho h/D}$ for an isotropic square plate.

Thickness-to-length ratio h/a	K_0	K_1	Method		
			Akhavan et al. [21]	Hassen Ait Atmane [22]	Present study
0.001	0	0	19.7391	19.7392	19.7320
	102	10	26.2112	26.2112	26.2048
	103	102	57.9961	57.9962	57.9894
0.1	0	0	19.0840	19.0658	19.0660
	102	10	25.6368	25.6236	25.5989
	103	102	57.3969	57.3923	57.2775
0.2	0	0	17.5055	17.4531	17.4553
	102	10	24.3074	24.2728	24.1068
	103	102	56.0359	56.0311	56.0260

Table 5
Comparison of non-dimensional natural frequencies $\overline{w} = \omega a^2 \sqrt{\rho h/D}$ for a simply supported isotropic square plate resting on an elastic foundation ($h/b = 0.2$).

K_0	K_1	$\widehat{\omega}_{11}$			$\widehat{\omega}_{12}$			$\widehat{\omega}_{13}$		
		Matsunaga [16]	Thai et al. [23]	Present	Matsunaga [16]	Thai et al. [23]	Present	Matsunaga [16]	Thai et al. [23]	Present
0	0	17.5260	17.4523	17.45533	38.4827	38.1883	38.2052	65.9961	65.3135	65.3731
10		17.7847	17.7248	17.7196	38.5929	38.3098	38.3203	66.0569	65.3841	65.4378
102		19.9528	20.0076	19.9413	39.5669	39.3895	39.3417	66.5995	66.0138	66.0178
103		34.3395	35.5039	35.1278	47.8667	48.8772	48.3829	71.5577	72.0036	71.5586
104		45.5260	45.5255	45.5260	71.9829	71.9829	71.98299	97.4964	101.7990	101.79922
105		45.5260	45.5255	45.5260	71.9829	71.9829	71.9829	101.7992	101.7990	101.7992
0	10	22.0429	22.2145	22.0950	43.4816	43.7943	43.5262	71.4914	71.9198	71.4814
10		22.2453	22.4286	22.3043	43.5747	43.9009	43.6274	71.5423	71.9839	71.5406
102		23.9830	24.2723	24.1068	44.3994	44.8445	44.5271	71.9964	72.5554	72.0713
103		36.6276	38.0650	37.6468	51.6029	53.3580	52.6856	76.1848	78.0290	77.1762
104		45.5260	45.5255	45.5260	71.9829	71.9829	71.9829	99.0187	101.7990	101.7992
105		45.5260	45.5255	45.5260	71.9829	71.9829	71.9829	101.7992	101.7990	101.7992

Table 6
Comparison of fundamental frequency parameter $\overline{w} = \omega b^2 \sqrt{SH/A}/\pi^2$ for homogeneous SSSS square plates ($a/b = 1$).

Thickness-to-length ratio h/a	Method	Fundamental frequency parameter			
Foundation stiffness parameters (K_0, K_1)		(100,0)	(500,0)	(100,10)	(500,10)
0.01	Hosseini-Hashemi [14]	2.2413	3.0215	2.6551	3.3400
	Mindlin theory [4]	2.2413	3.0215	2.6551	3.3400
	3D method [5]	2.2413	3.0214	2.6551	3.3398
	Present	2.2413	3.0214	2.6551	3.3399
Foundation stiffness parameters (K_0, K_1)		(200,0)	(1000,0)	(200,10)	(1000,10)
0.1	Hosseini-Hashemi [14]	2.3989	3.7212	2.7842	3.9805
	Mindlin theory [4]	2.3989	3.7212	2.7842	3.9805
	3D method [5]	2.3951	3.7008	2.7756	3.9566
	Present	2.3971	3.7153	2.7811	3.9738
Foundation stiffness parameters (K_0, K_1)		(0,10)	(10,10)	(100,10)	(1000,10)
0.2	Hosseini-Hashemi [14]	2.2505	2.2722	2.4590	3.8567
	Mindlin theory [4]	2.2505	2.2722	2.4591	3.8567
	3D method [5]	2.2334	2.2539	2.4300	3.7111
	Present	2.2386	2.2599	2.4425	3.8144

In Fig. 5, the variations of non-dimensional fundamental frequencies $\overline{w} = \omega b^2 \sqrt{SH/A}/\pi^2$ of simply supported Al/Al_2O_3 functionally graded square plates with respect to the thickness-to-length ratio $\delta = h/a$ are plotted. It is seen from the figure that increasing the value of the Winkler coefficient of foundation causes an increase in the fundamental frequency.

5. Conclusions

In this work, an efficient new refined shear deformation theory based on the neutral surface concept was effectively used to study extensively the free vibration analysis of an FG simply-supported plate resting on elastic foundations using an analytical procedure. Equilibrium equations are obtained using Hamilton's principle. The Navier method is used for the ana-

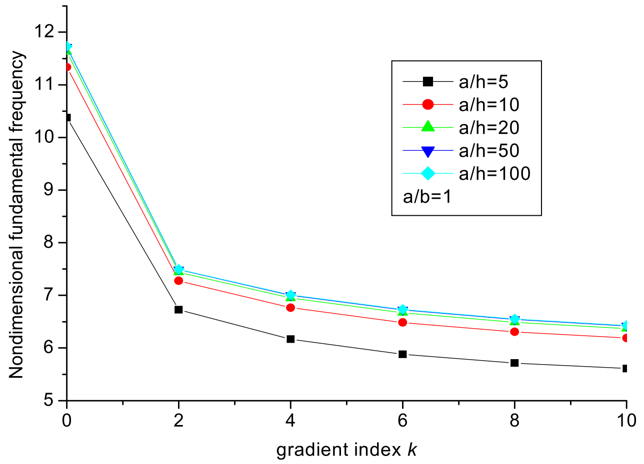

Fig. 2. Non-dimensional fundamental frequency $\overline{w} = \omega a^2/h\sqrt{\rho_m/E_m}$ of Al/Al_2O_3 as a function of the power-law index k.

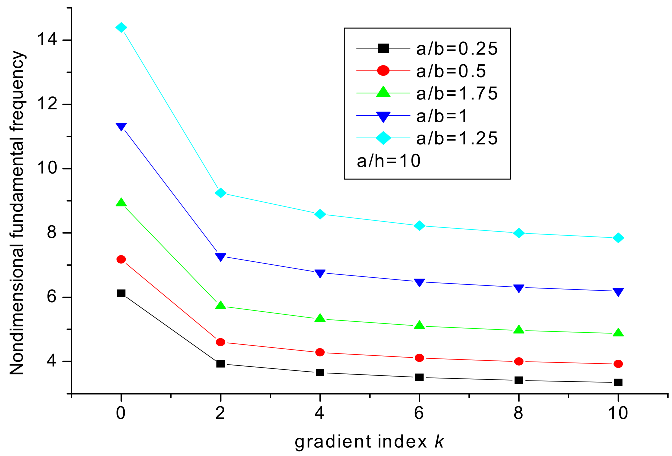

Fig. 3. Non-dimensional fundamental frequency $\overline{w} = \omega a^2/h\sqrt{\rho_m/E_m}$ of Al/Al_2O_3 as a function of the power-law index k.

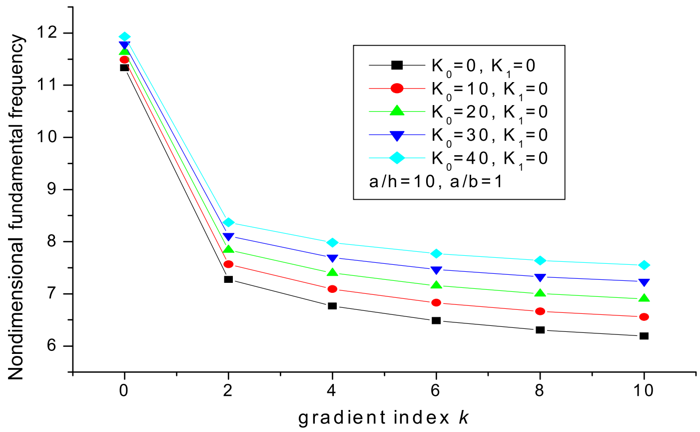

Fig. 4. Non-dimensional fundamental frequency $\overline{w} = \omega a^2/h\sqrt{\rho_m/E_m}$ of Al/Al_2O_3 resting on a Winkler foundation as a function of the power-law index k.

lytical solutions of the functionally graded plate with simply supported boundary conditions. It was demonstrated that the present solution is highly efficient for an exact analysis of the vibration of FG rectangular plates on the elastic foundations. Parametric studies for making the power-law index, the foundation stiffness parameters, the aspect and side-to-thickness ratios vary are discussed and demonstrated through illustrative numerical examples. The present findings will be a useful benchmark for evaluating other analytical and numerical methods

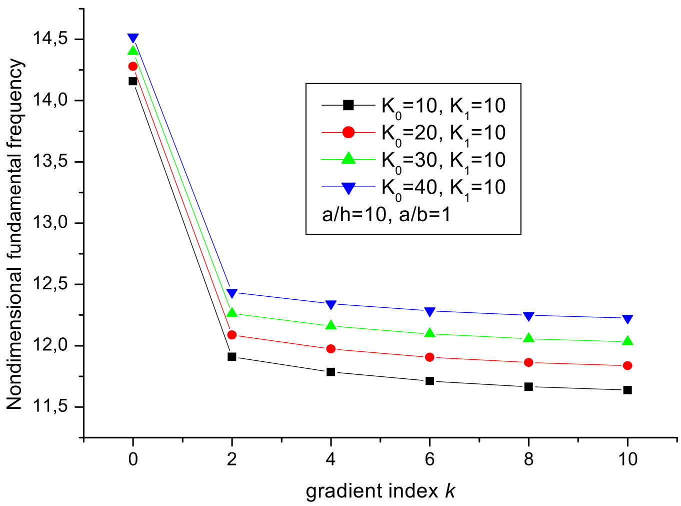

Fig. 5. Non-dimensional fundamental frequency $\overline{w} = \omega a^2/h\sqrt{\rho_m/E_m}$ of Al/Al$_2$O$_3$ resting on an elastic foundation as a function of the power-law index k.

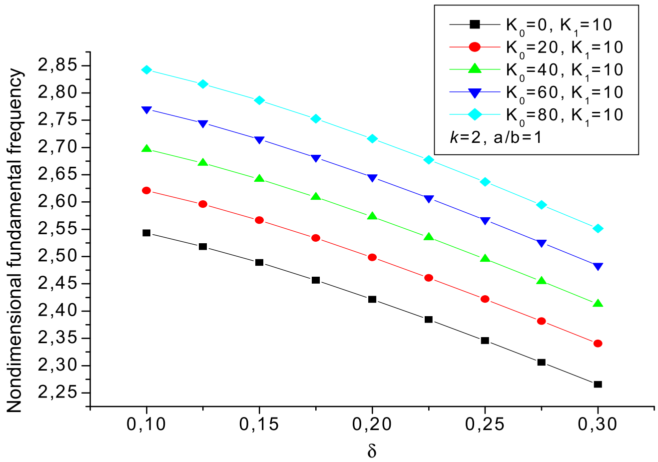

Fig. 6. Non-dimensional fundamental frequency $\overline{w} = \omega b^2\sqrt{SH/A}/\pi^2$ of Al/Al$_2$O$_3$ resting on an elastic foundation as a function of the thickness-to-length ratio ($\delta = h/a$).

References

[1] M. Koizumi, FGM activities in Japan, Composites, Part B, Eng. 28B (1997) 1–4.
[2] A.D. Kerr, Elastic and viscoelastic foundation models, ASME J. Appl. Mech. 31 (3) (1964) 491–498.
[3] P.L. Pasternak, On a New Method of Analysis of an Elastic Foundation by Means of Two Foundation Constants, Gosudarstvennoe Izdatelstvo Literaturi po Stroitelstvu i Arkhitekture, Moscow, USSR, 1954, pp. 1–56.
[4] Y. Xiang, C.M. Wang, S. Kitipornchai, Exact vibration solution for initially stressed Mindlin plates on Pasternak foundation, Int. J. Mech. Sci. 36 (1994) 311–316.
[5] D. Zhou, Y.K. Cheung, S.H. Lo, F.T.K. Au, Three-dimensional vibration analysis of rectangular thick plates on Pasternak foundations, Int. J. Numer. Methods Eng. 59 (10) (2004) 1313–1334.
[6] J.N. Reddy, Analysis of functionally graded plates, Int. J. Numer. Methods Eng. 47 (2000) 663–684.
[7] Senthil S. Vel, R.C. Batra, Exact solution for thermoelastic deformations of functionally graded thick rectangular plates, AIAA J. 40 (7) (2002).
[8] Mohammad Talha, B.N. Singh, Static response and free vibration analysis of FGM plates using higher order shear deformation theory, Appl. Math. Model. 34 (2010) 3991–4011.
[9] A.J.M. Ferreira, R.C. Batra, C.M.C. Roque, L.F. Qian, P.A.L.S. Martins, Static analysis of functionally graded plates using third-order shear deformation theory and a meshless method, Compos. Struct. 69 (2005) 449–457.
[10] F. Ramirez, P.R. Heyliger, E. Pan, Static analysis of functionally graded elastic anisotropic plates using a discrete layer approach, Composites, Part B, Eng. 37 (2006) 10–20.
[11] Jae-Sang Park, Ji-Hwan Kim, Thermal postbuckling and vibration analyses of functionally graded plates, J. Sound Vib. 289 (2006) 77–93.
[12] G.N. Praveen, J.N. Reddy, Nonlinear transient thermoelastic analysis of functionally graded ceramic–metal plates, Int. J. Solids Struct. 35 (1998) 4457–4476.
[13] D.G. Zhang, Y.H. Zhou, A theoretical analysis of FGM thin plates based on physical neutral surface, Comput. Mater. Sci. 44 (2008) 716–720.
[14] S. Hosseini-Hashemi, M. Fadaee, H. Rokni Damavandi Taher, Exact solutions for free flexural vibration of Lévy-type rectangular thick plates via third-order shear deformation plate theory, Appl. Math. Model. 35 (2011) 708–727.

[15] D. Zhou, Y.K. Cheung, F.T.K. Au, S.H. Lo, Three-dimensional vibration analysis of thick rectangular plates using Chebyshev polynomial and Ritz method, Int. J. Solids Struct. 39 (2002) 6339–6353.
[16] H. Matsunaga, Free vibration and stability of functionally graded plates according to a 2-D higher-order deformation theory, Compos. Struct. 82 (2008) 499–512.
[17] A.W. Leissa, The free vibration of rectangular plates, J. Sound Vib. 31 (3) (1973) 257–293.
[18] F.L. Liu, K.M. Liew, Analysis of vibrating thick rectangular plates with mixed boundary constraints using differential quadrature element method, J. Sound Vib. 225 (5) (1999) 915–934.
[19] X. Zhao, Y.Y. Lee, K.M. Liew, Free vibration analysis of functionally graded plates using the element-free kp-Ritz method, J. Sound Vib. 319 (2009) 918–939.
[20] S.S. Akavci, An efficient shear deformation theory for free vibration of functionally graded thick rectangular plates on elastic foundation, Compos. Struct. 108 (2014) 667–676.
[21] H. Akhavan, Sh. Hosseini Hashemi, H. Rokni Damavandi Taher, A. Alibeigloo, Sh. Vahabi, Exact solutions for rectangular Mindlin plates under in-plane loads resting on Pasternak elastic foundation. Part II: frequency analysis, Comput. Mater. Sci. 44 (2009) 951–961.
[22] A. Hassen, T. Abdelouahed, M. Ismail, A.B. El Abbas, Free vibration analysis of functionally graded plates resting on Winkler–Pasternak elastic foundations using a new shear deformation theory, Int. J. Mech. Mater. Des. 6 (2010) 113–121.
[23] H.T. Thai, D.H. Choi, A refined shear deformation theory for free vibration of functionally graded plates on elastic foundation, Composites, Part B, Eng. 43 (2012) 2335–2347.